Nature of S · · · · O Interaction in Short X–S · · · · O Contacts: Charge Density Experimental Studies and Theoretical Interpretation

Claudine Cohen-Addad *
Laboratoire de Spectrométrie Physique, Université Scientifique et Médicale de Grenoble, B.P. 68, 38402 St. Martin d'Hères Cedex, France
Mogens S. Lehmann and Pierre Becker
Institut Laue-Langevin, 156X Centre de Tri, 38042 Grenoble Cedex, France
László Párkányi and Alajos Kálmán
Central Research Institute for Chemistry, Hungarian Academy of Sciences, Budapest, POB 17, H-1525 Hungary

2-(2-Chlorobenzoylimino)-1,3-thiazolidine (I) and 3-benzoylimino-4-methyl-1,2,4-oxathiazane (II) present short intramolecular S · · · · O contacts of 2.68 and 2.24 Å, respectively. *X*-Ray and neutron diffraction at 122 K performed on (II), for comparison with (I), already studied, led to experimental charge density deformation maps which exhibit a strong peak around the sulphur atom. Using simple molecular orbital theory, it is possible to interpret the shortening of S · · · · O distances in these compounds by σ-type interaction between the oxygen *p* and the sulphur *p* and *d* orbitals. The significant variation of the equilibrium S · · · · O distance with the nature of the atom bonded to S is explained in terms of the strength of the coupling between X–S antibonding orbital and oxygen lone-pair orbitals.

In recent years the atomic configuration X–S · · · · O=C has been observed on many occasions.[1] The distances between S and O, found from structure analysis, range from 2.03 to 2.96 Å, which in all cases is considerably less than the sum of the van der Waals radii of 3.3 Å. Several theoretical interpretations of this interaction have been brought forward. From extended Hückel calculations including compounds with S · · · · O distances of between 2.41 and 2.64 Å the conclusion was that no covalent interaction existed between the atoms, whereas a study of compounds with distances in the range 2.18—2.41 using CNDO methods showed an interaction where the *p* and *d* orbitals in particular of S were involved.[2–4]

In addition, an experimental study using combined *X*-ray and neutron-diffraction data was carried out on 2-(2-chlorobenzoylimino)-1,3-thiazolidine (I), in which the S · · · · O length is 2.68 Å.[5] The deformation electron density showed no trace of electrons in the region between S and O and all deformation peaks around the atoms could be attributed to lone pairs of the two atoms [Figure 2(a)]. 3-Benzoylimino-4-methyl-1,2,4-oxathiazane (II) has a much shorter S · · · · O contact of 2.25 Å.[6] It was therefore felt that the probability of finding changes of density in the region of interest would be higher, and this led us to undertake the present study. Moreover, in order to rationalize our findings we undertook a series of calculations using a simple theoretical approach employing extended Hückel calculations. Although these methods are clearly only able to give qualitative insight, they should, together with the already available studies, allow us to discern the driving forces between these interactions.

Results and Discussion

X-Ray and Neutron Diffraction Studies at 122 K.—Both sets of data were collected at a temperature of 122 K. In order to ensure the correct setting a calibration was carried out using a crystal of KH_2PO_4. This compound has a phase transition at 122.4 K, which is easily identifiable from the intensity overshoot in strong, low-order reflections due to the reduction of secondary extinction at the transition point.

X-Ray data. The *X*-ray data were measured on the Philips PW1100 four-circle diffractometer from 'Groupement Grenoblois de Diffractométrie,' C.N.R.S., Grenoble. The crystal (0.2 × 0.25 × 0.3 mm³) was cooled using a nitrogen gas-flow system. The unit cell was determined from 20 reflections and the values obtained were $a = 7.278(6)$, $b = 10.978(8)$, $c = 14.600(13)$ Å, $\beta = 114.1(1)°$. The space group is $P2_1/c$. The data were recorded using an ω scan technique in the background-peak-background mode. The peak width was fixed from step recording of strong reflections. Crystal-monochromatized Mo-radiation was used and the limiting $\sin\theta/\lambda$ was 0.85 Å^{-1}, giving 6 487 reflections. After averaging there were 4 099 reflections of which 2 428 had intensities of more than three times their standard deviation.

Neutron data. Neutron data were recorded on the D8 diffractometer of the Institut Laue-Langevin using a wavelength of 0.897 Å and employing an ω–2θ step-scan technique using 41 step and variable step-lengths. The crystal was cooled using a closed-loop refrigerator.[7] Data were reduced to intensities using the minimal $\sigma I/I$ method with correction for the known bias in the method.[8] All 5 202 sets of data were collected up to a $\sin\theta/\lambda$ of 0.72 Å^{-1}, giving 3 611 reflections after averaging. The crystal volume was 2.8 mm³ and the shape was almost spherical. It was thus deemed unnecessary to do any absorption correction. Moreover, the intensity was measured for a series of reflections for various orientations around the scattering vector, and in all cases the intensity remained constant. This also indicated that any extinction effect was isotropic.

Structure refinement and electron deformation densities. Atomic co-ordinates and thermal motion were obtained using a conventional least-squares technique, using as observations the squared amplitudes, F^2. The weights were $1/[\sigma^2(F^2) + (0.05\ F^2)^2]$ for the *X*-rays, and in the neutron case $w = 1/[\sigma^2(F^2) + (0.03\ F^2)^2]$ was used. The $\sigma(F^2)$ was derived from counting statistics. The computer programs XFLS and LINEX[9,10] were used for *X*-ray and neutron measurements, respectively, and a correction for isotropic extinction was included in the neutron case. This proved to be negligible. Form factors for the atoms for *X*-rays were taken from International Tables, and for the neutrons the recent compilation of Koester and Rauch was used for the scattering lengths.[11] Final *R*-values were $R = \Sigma|F_o - F_c|/\Sigma|F_o|$, 0.041 for *X*-rays and 0.037 for neutrons. The lists of neutron and *X*-ray structure factors, the *X*-ray and neutron parameters, and the equation of mean planes have been deposited [Sup-

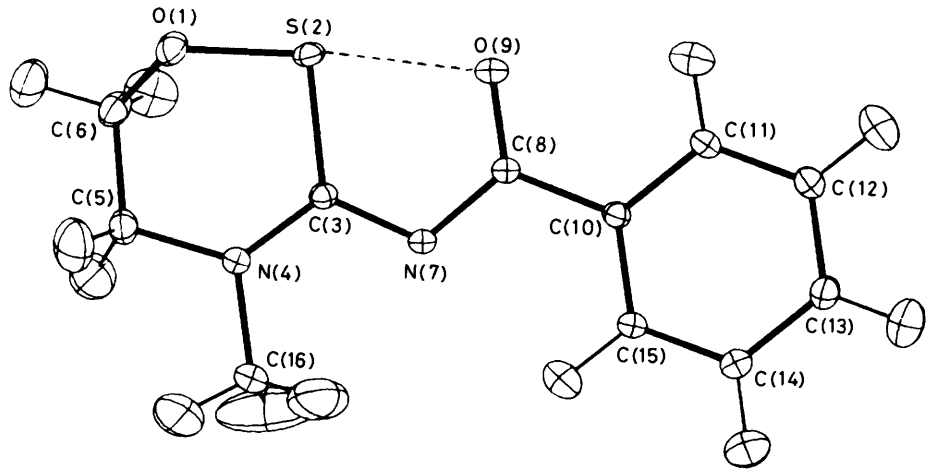

Figure 1. 3-Benzoylimino-4-methyl-1,2,4-oxathiazane projection of the molecule in the S(2)–N(7)–O(9) plane

plementary Publication No. SUP 23761 (35 pp.)*]. All the calculations were carried out on the PDP10 at the Institut Laue-Langevin, Grenoble.

The general agreement between the thermal parameters obtained from *X*-rays and neutrons was good, but showed, as is commonly observed, that the thermal parameters for the non-hydrogen atoms from neutron measurements were generally smaller than *X*-ray observations; some of this can be attributed to bonding effects. As the angular range of the *X*-ray data was limited, it was not possible to carry out calculations using only high-order *X*-ray data, which were unaffected by bonding effects and in the following calculations of deformation electron densities it was then assumed that there were no differences between the thermal parameters. These deformation maps were therefore obtained as a difference between the total experimental electron density and a model density calculated from spherical independent atoms whose atomic and thermal parameters are those obtained by neutron diffraction. The common scale factor was obtained by a least-squares calculation using the observed *X*-ray data up to $\sin\theta/\lambda = 0.75$. Only the scale factor was varied and the atomic parameters came from the neutron refinement. The error in the electron density, away from the atoms, is typically between 0.05 and 0.1 e Å^{-3}.

Results. Figure 1 shows the projection of the molecule in the plane formed by S–N(7)–O(9).[12] Neutron-diffraction results have been used. The central part of the molecule is virtually a plane: the benzoyl plane forms an angle of 6.0(1)° with the S–C(3)–N(7)–C(8)–O(9) plane. We found no significant differences between the geometrical parameters obtained by neutrons given in Table 1 and *X*-rays at low or at room temperatures. Figure 2 shows the X–N deformation density in the region of the S · · · · O contact for compound (II) in comparison with the previously studied molecule (I). The weak peak near O(9), weaker in (II) than in (I), is particularly noticeable. This is supposedly the lone pair of oxygen. If we introduce in our calculation an sp^2 deformation in the model for the calculated density of oxygen [13] this peak disappears almost completely. On the other hand we find in (II) a very large peak in the density near S, and in this case we cannot explain this by modelling it with an sp^2 deformation. Indeed most of the peak remains if an sp^2 deformed density is subtracted.

* For details of the Supplementary Scheme see Instructions for Authors (1984), *J. Chem. Soc., Perkin Trans. 2*, 1984, Issue 1.

Energy Calculations with the Extended Hückel Method.—Models. The two molecules that have been studied experimentally are far too complicated for any quantitative theoretical investigation. We first tried to see which chemical simplifications could be made that do not perturb the interesting X–S · · · · O region. Therefore, we performed test calculations with the extended Hückel method [14] (*d*-orbitals were included for sulphur atoms). We observed that the density matrix was not altered significantly when replacing the molecules by the models shown in Figure 3. Such model molecules still contain too many atoms for a quantitative *ab initio* study to be reasonable.

Since we observed from the experimental geometries that heavy atoms concerned in Figure 3 are not far from being coplanar (Table 1 in ref. 6) we further assumed planar configurations in the following calculations. Distances and angles were kept as close as possible to the experimental geometries. In (I) we were obliged, for steric reasons, to fix the angle C(1)–S–C(3) at 120° instead of the experimental value of 91°. Such constraints were not necessary for (II). The Cartesian frame is sketched in Figure 3. The atomic numbering of Figure 3 is the same as that of Figures 1 and 2.

Results. The S · · · · O distance was varied by slight changes in the S–C(3)–N(7) and O(9)–C(8)–N(7) angles. Energy results for molecules (I) and (II) are shown in Figure 4 where a minimum is observed in both cases, corresponding to a distance in reasonable agreement with the experimental observations. For the short interaction case we also did calculations where we discarded the S · · · · O interactions: this was accomplished by putting the overlap and therefore the Hamiltonian elements between S and O(9) equal to zero. The resulting energy curve is shown by the dashed line of Figure 4(b). It is apparent that, energetically, the S · · · · O coupling results in a repulsive interaction. In Table 2 we give the elements of the density matrix that are relevant to the X–S · · · · O region and that are significantly different from zero. The main difference concerns the S · · · · O interaction where molecule (II) shows a significant bond coupling, which is essentially of σ-type between *p*,*d*-sulphur and *p*-oxygen orbitals. In particular, the comparison of S · · · · O(9) with the normal covalent S–O(1) covalent bond is easily seen in Table 4 and is also depicted by the two bond orders of 0.2 and 0.76, respectively. On the other hand, the S–C(3) and C(8)–O(9) couplings are similar in the two compounds (see Table 2). Both bonds are of mixed σ- and π-types.

The σ-type bonding in the S · · · · O(9) interaction of

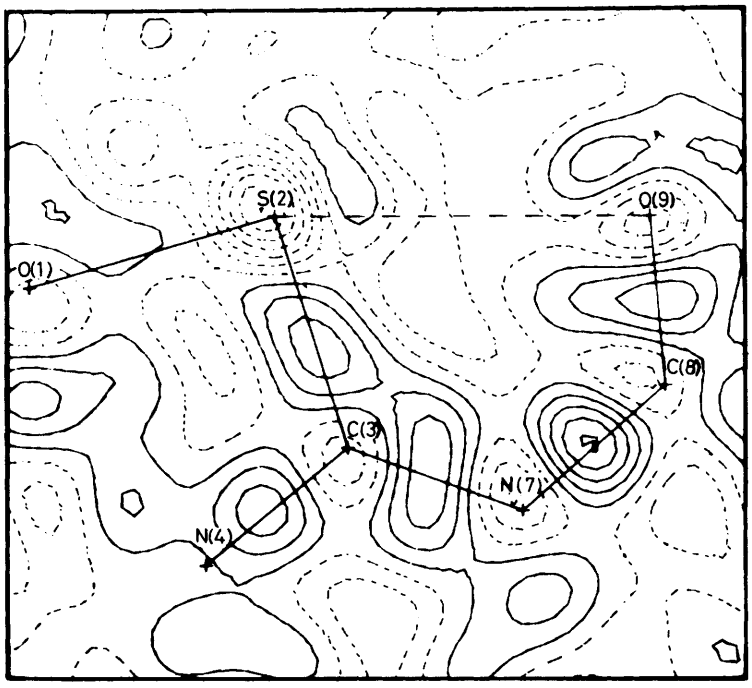

a

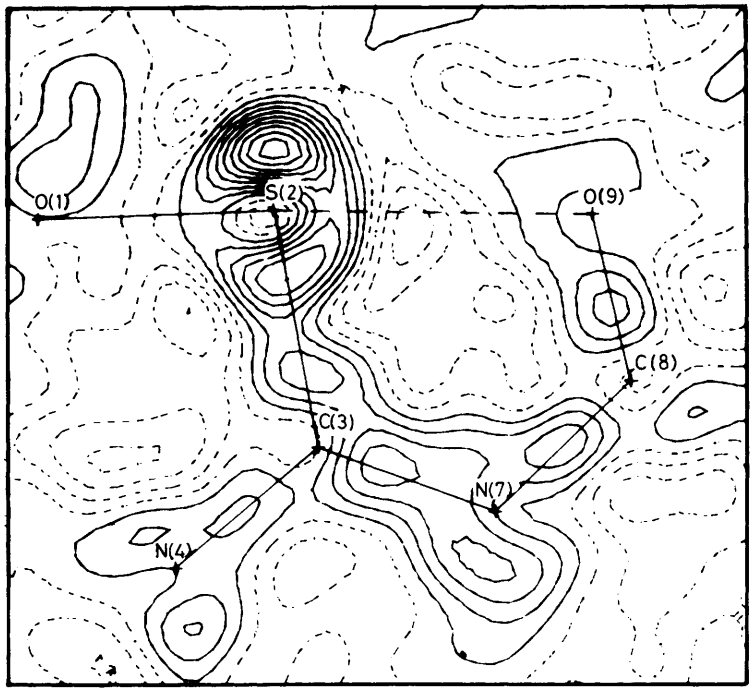

b

Figure 2. (X–N) deformation-density map in the S(2)–N(7)–O(9) plane. (a) 2-(2-Chlorobenzoylimino)-1,3-thiazolidine (I); and (b) 3-benzoylimino-4-methyl-1,2,4-oxathiazane (II), levels are at 0.1 e Å^{-3}, negative contours are broken

molecule (II) is the result of the competition of two contributions.

(i) A strong repulsion between the two overlapping electron clouds; this can be seen from a calculation where we put the Hamiltonian $\mathscr{H}$[S · · · · O(9)] equal to zero and the overlap $\mathscr{S}$[S · · · · O(9)] different from zero. In this case a strongly repulsive coupling appears in the density matrix (of the order of 0.6).

(ii) An attractive contribution owing to the Hamiltonian matrix elements $\mathscr{H}$[S · · · · O(9)].

Table 1. 3-Benzoylimino-4-methyl-1,2,4-oxathiazane: bond lengths and angles from neutron-diffraction data at 122 K, with e.s.d.s in parentheses

Bond	Length (Å)	Bond	Length (Å)
O(1)–S(2)	1.685(3)	N(4)–C(16)	1.462(1)
O(1)–C(6)	1.429(1)	C(5)–C(6)	1.505(2)
S(2)–C(3)	1.770(2)	C(5)–H′(5)	1.096(3)
S(2)–O(9)	2.245(3)	C(5)–H″(5)	1.098(2)
C(3)–N(4)	1.333(2)	C(6)–H′(6)	1.101(4)
C(3)–N(7)	1.335(2)	C(6)–H″(6)	1.103(3)
N(4)–C(5)	1.466(2)	N(7)–C(8)	1.349(1)
C(8)–O(9)	1.252(2)	C(12)–H(12)	1.090(3)
C(8)–C(10)	1.485(2)	C(13)–C(14)	1.396(1)
C(10)–C(11)	1.400(1)	C(13)–H(13)	1.090(4)
C(10)–C(15)	1.401(2)	C(14)–C(15)	1.391(2)
C(11)–C(12)	1.393(2)	C(14)–H(14)	1.086(3)
C(11)–H(11)	1.084(3)	C(15)–H(15)	1.088(3)
C(12)–C(13)	1.398(2)	C(16)–H′(16)	1.066(4)
		C(16)–H″(16)	1.063(4)
		C(16)–H‴(16)	1.053(5)

Bond	Angle (°)	Bond	Angle (°)
S(2)–O(1)–C(6)	112.8(2)	O(1)–C(6)–H′(6)	108.2(3)
O(1)–S(2)–C(3)	98.5(2)	O(1)–C(6)–H″(6)	109.8(3)
O(1)–S(2)–O(9)	173.2(3)	C(5)–C(6)–H′(6)	110.4(3)
C(3)–S(2)–O(9)	78.9(2)	C(5)–C(6)–H″(6)	110.8(3)
S(2)–C(3)–N(4)	121.2(2)	H′(6)–C(6)–H″(6)	109.3(4)
S(2)–C(3)–N(7)	120.6(2)	C(3)–N(7)–C(8)	114.4(2)
N(4)–C(3)–N(7)	118.2(2)	N(7)–C(8)–O(9)	122.3(2)
C(3)–N(4)–C(5)	126.5(2)	N(7)–C(8)–C(10)	117.5(2)
C(3)–N(4)–C(16)	119.5(2)	O(9)–C(8)–C(10)	120.1(2)
C(5)–N(4)–C(16)	113.8(2)	S(2)–O(9)–C(8)	103.1(2)
N(4)–C(5)–C(6)	112.6(2)	C(8)–C(10)–C(11)	119.0(2)
N(4)–C(5)–H′(5)	108.4(3)	C(8)–C(10)–C(15)	121.0(2)
N(4)–C(5)–H″(5)	107.8(3)	C(11)–C(10)–C(15)	119.9(2)
C(6)–C(5)–H′(5)	110.4(3)	C(10)–C(11)–C(12)	120.0(2)
C(6)–C(5)–H″(5)	110.0(3)	C(10)–C(11)–H(11)	119.2(3)
H′(5)–C(5)–H″(5)	107.5(4)	C(12)–C(11)–H(11)	120.8(3)
O(1)–C(6)–C(5)	108.4(2)	C(11)–C(12)–C(13)	119.8(2)
C(11)–C(12)–H(12)	120.6(3)	C(10)–C(15)–H(15)	119.2(3)
C(13)–C(12)–H(12)	119.6(3)	C(14)–C(15)–H(15)	120.9(3)
C(12)–C(13)–C(14)	120.2(2)	N(4)–C(16)–H′(16)	110.8(4)
C(12)–C(13)–H(13)	119.9(3)	N(4)–C(16)–H″(16)	109.5(4)
C(14)–C(13)–H(13)	119.9(3)	N(4)–C(16)–H‴(16)	111.1(5)
C(13)–C(14)–C(15)	120.1(2)	H′(16)–C(16)–H″(16)	108.7(6)
C(13)–C(14)–H(14)	120.4(3)	H″(16)–C(16)–H‴(16)	107.7(7)
C(15)–C(14)–H(14)	119.5(3)	H′(16)–C(16)–H‴(16)	108.9(7)
C(10)–C(15)–C(14)	119.9(2)		

Bond	Torsion angle (°)
N(4)–C(3)–S(2)–O(1)	9.8(2)
N(4)–C(5)–C(6)–O(1)	−50.4(2)
C(5)–N(4)–C(3)–S(2)	10.0(2)
C(5)–C(6)–O(1)–S(2)	76.3(2)
C(6)–O(1)–S(2)–C(3)	−51.9(2)
C(6)–C(5)–N(4)–C(3)	8.2(2)
N(7)–C(3)–S(2)–O(1)	−168.2(2)
N(7)–C(3)–N(4)–C(5)	−171.9(2)
N(7)–C(8)–O(9)–S(2)	8.9(3)
C(8)–N(7)–C(3)–S(2)	−2.5(2)
C(8)–N(7)–C(3)–N(4)	179.4(2)
C(13)–C(12)–C(11)–C(10)	−0.2(2)
C(13)–C(14)–C(15)–C(10)	−0.4(2)
C(14)–C(13)–C(12)–C(11)	0.2(2)
C(14)–C(15)–C(10)–C(8)	−176.5(2)
C(14)–C(15)–C(10)–C(11)	0.3(2)
C(8)–O(9)–S(2)–O(1)	60.2(2)
C(8)–O(9)–S(2)–C(3)	−7.5(2)
O(9)–S(2)–O(1)–C(6)	−118.4(23)
O(9)–S(2)–C(3)–N(4)	−176.6(2)
O(9)–S(2)–C(3)–N(7)	5.4(1)

Table 1 *(continued)*

Bond	Torsion angle (°)
O(9)–C(8)–N(7)–C(3)	−5.9(2)
C(10)–C(8)–N(7)–C(3)	172.3(2)
C(10)–C(8)–O(9)–S(2)	−169.2(4)
C(11)–C(10)–C(8)–N(7)	178.0(2)
C(11)–C(10)–C(8)–O(9)	−3.8(2)
C(12)–C(11)–C(10)–C(8)	176.9(2)
C(15)–C(10)–C(8)–O(9)	173.1(2)
C(15)–C(10)–C(11)–C(12)	0.0(2)
C(15)–C(14)–C(13)–C(12)	0.1(2)
C(16)–N(4)–C(3)–S(2)	−174.9(3)
C(16)–N(4)–C(3)–N(7)	3.2(2)

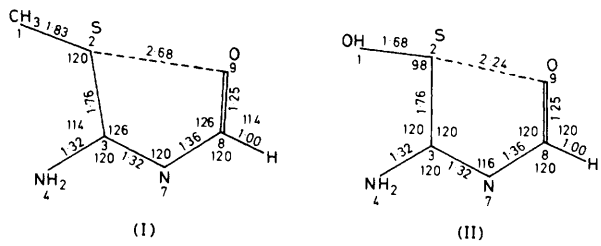

Figure 3. Model molecules (I) and (II) used in energy calculations. Cartesian frame: the molecules in the plane (xy), axis (x) parallel to S · · · · O(9)

Table 2. Significant coefficients of density matrix in the X–S · · · · O region for model molecules (I) and (II) at equilibrium

Model (I)			
p_x(S)–p_x[O(9)]	−0.001	p_y(S)–p_y[C(3)]	−0.43
$d_{x^2-y^2}$(S)–p_x[O(9)]	−0.15	p_z(S)–p_z[C(3)]	0.36
p_x(S)–p_x[C(1)]	−0.03	p_y[O(9)]–p_y[C(8)]	−0.33
d_{xz}(S)–p_z[C(1)]	−0.09	p_z[O(9)]–p_z[C(8)]	0.41
Model (II)			
p_x(S)–p_x[O(9)]	−0.26	d_{xy}(S)–p_y[O(1)]	−0.22
$d_{x^2-y^2}$(S)–p_x[O(9)]	−0.29	d_{xz}(S)–p_z[O(1)]	−0.32
d_{z^2}(S)–p_x[O(9)]	0.13	p_y(S)–p_y[C(3)]	−0.42
p_x(S)–p_x[O(1)]	−0.5	p_z(S)–p_z[C(3)]	0.37
p_z(S)–p_z[O(1)]	−0.08	p_y[O(9)]–p_y[C(8)]	−0.32
$d_{x^2-y^2}$(S)–p_x[O(1)]	0.12	p_z[O(9)]–p_z[C(8)]	0.42

The overlap coefficients of S—O(1) and S · · · · O(9) in (II) have a ratio of 2 (−0.5 and −0.22, respectively) but the bond orders have a ratio of 3.8 (0.76 and 0.2, respectively).

In molecule (I), the S · · · · O(9) interaction is small, though there exists a significant σ bond coupling between orbitals $d_{x^2-y^2}$(S) and p_x[O(9)]. This could justify the short experimental value of 2.68Å for the S · · · · O(9) distance compared with the sum of the van der Waals radii, 3.3 Å.

When we vary the S · · · · O(9) distance (D) we observe that only the S · · · · O(9) part of the density matrix is significantly modified. In Table 3 the most significant coefficients are reported for various values of D. Even for D in molecule (II), equal to the equilibrium value of D in molecule (I), the S · · · · O(9) bonding character is much more pronounced in (II) than in (I). Conversely, even going to very short distances in (I), the S · · · · O(9) bonding character remains very small.

Discussion. It is obvious that the difference between the two cases arises from the nature of the atom adjacent to S. We thus restrict the discussion to the X–S · · · · O part. Two situations may occur.

Table 3. Significant coefficients of density matrix in the S · · · · O part as a function of the S · · · · O distance, *D*, for model molecules (I) and (II)

Model (I)							
p_x[O(9)]	*D*/Å						
S	2.28	2.38	2.47	2.58	2.68	2.78	2.88
p_x	−0.02	−0.01	0.009	0.005	−0.001	−0.003	−0.005
$d_{x^2-y^2}$	−0.26	−0.24	−0.19	−0.18	−0.15	−0.13	−0.11
d_{z2}	0.14	0.13	0.1	0.08	0.07	0.06	0.05
Model (II)							
p_x[O(9)]	*D*/Å						
S	2.04	2.14	2.24	2.34	2.45	2.55	2.65
p_x	−0.30	−0.28	−0.26	−0.23	0.19	−0.16	−0.14
$d_{x^2-y^2}$	−0.28	−0.30	−0.29	−0.26	−0.23	−0.21	−0.18
d_{z2}	0.12	0.13	0.13	0.12	0.11	0.09	0.08

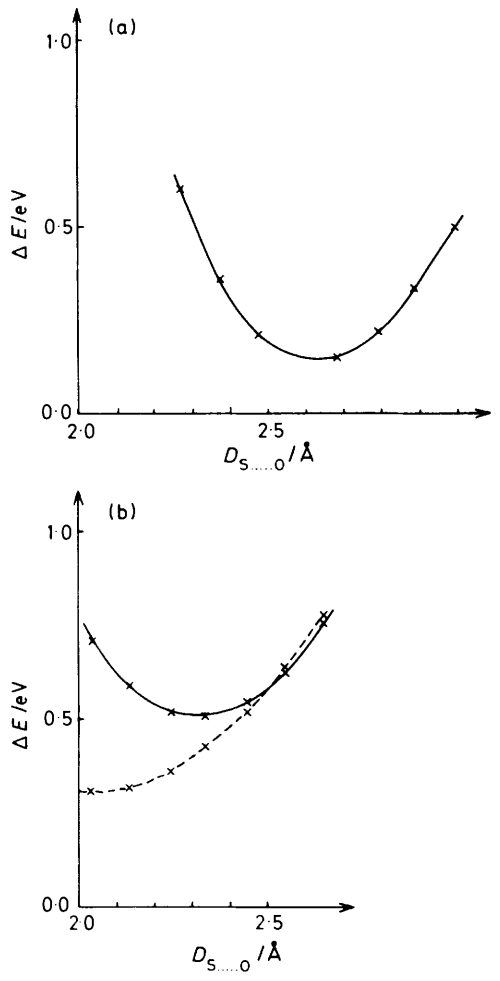

Figure 4. Energy curves as a function of S · · · · O distance calculated in model molecules (I) and (II), (a) and (b), respectively

(a) X More electronegative than S (X = O). X–S coupling leads to two localized orbitals, one bonding orbital which is lower than the X level, and an anti-bonding orbital ψ^*, which is higher than the S level (see Appendix). If the gap between the lone pair orbital of O(9), ψ_{LP}, and ψ^* is small enough, for example if X = O, a coupling can exist between ψ_{LP} and ψ^* resulting in a bonding interaction and a charge transfer to the X–S region from the lone pair of O(9).

Table 4. Mulliken populations of X–S · · · · O part in model molecules (I) and (II) at equilibrium S · · · · O distances

Model I. Bond order S · · · · O(9) = 0.03

Atom	Orbital *s*	p_x	p_y	p_z	Net charge (e)
S	1.49	1.26	1.37	1.80	−0.19
O(9)	1.75	1.43	1.70	1.76	−1.15
C(1)	1.20	0.90	0.96	0.97	−0.03

Model II. Bond orders S · · · · O(9) = 0.20, S–O(1) = 0.76

Atom	Orbital *s*	p_x	p_y	p_z	Net charge (e)
S	1.52	0.62	1.43	1.80	0.06
O(9)	1.74	1.75	1.70	1.75	−0.44
O(1)	1.74	1.41	1.65	1.86	−0.66

(b) X Less electronegative than S (X = C). The gap between ψ_{LP} of O(9) and ψ^* is much higher and no coupling occurs.

The two possibilities and more quantitative arguments are given in the Appendix.

However, in both cases, as observed from the previous discussion, the *d*-orbitals of S play a significant role and the interaction between *p*-levels of O(9) and *d*-levels of S are responsible for an extra bonding character that is present in both compounds.

In the case where there is a $\psi^*\psi_{LP}$ interaction the coupling is essentially of a σ-type, which explains why *sp* hybridization is less pronounced in (II) than in (I) and therefore the lone pairs of X–S · · · · O are more of *p* character in (II) than in compound (I) as observed experimentally.

If we look at the various contributions to the net Mulliken populations in S and O(9) for the two compounds (Table 4), we observe that the density localized around sulphur is much more anisotropic in (II) than in (I) and there is a very significant reversal of p_x and p_y contributions for the two compounds. Similarly, the anisotropy observed in the deformation densities is much higher for (II) than for (I), so qualitatively there is agreement between calculations and observations. We cannot, however, at this level of calculation hope for any detailed quantitative agreement.

Appendix

Justification of the X–S · · · · O *interaction.*—We make some simplifying assumptions. First, X, S, and O are supposed to be collinear. The S · · · · O distance is fixed at the equilibrium value for (II), X = OH, *i.e.*, 2.24 Å. For compound (I), X = CH_3.

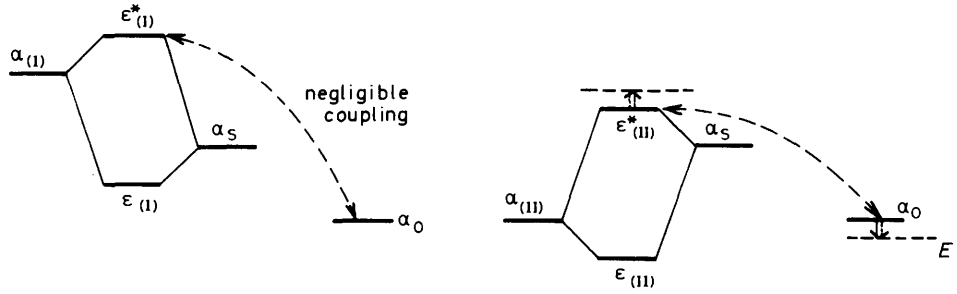

Figure 5. Summary of results

The energy difference between the *s*-states of sulphur and oxygen (10 eV) allows one to limit the discussion to p_σ-type interactions. For oxygen we will consider the *p* orbitals rather than the lone pair hybridized orbital.

Let $\alpha_i = \langle p_i|H|p_i\rangle$

We observe that

$$\alpha_{(I)} \# \alpha_S - 2\delta$$

$$\alpha_{(II)} = \alpha_o \# \alpha_S - 2\delta$$

where δ *ca.* 1 eV.

From the calculations we have $\langle p_i|p_S\rangle$ *ca.* 0.3. This allows us, to a first approximation, to neglect the overlap in the wave functions. From our computations and the values of X–S bond energies, we may consider the resonance integral

$$-\beta = \langle p_i|H|p_S\rangle$$

identical for the two compounds.

From the observation that $\langle p_S|p_o\rangle$ *ca.* 0.15, we finally assume

$$\langle p_S|H|p_o\rangle = -\beta/2$$

It is now trivial to construct the bonding and antibonding molecular orbitals for X–S. We define the angle θ through

$$\cos 2\theta = \delta/\sqrt{\delta^2 + \beta^2}$$

and we call *D* the quantity

$$D = 2\sqrt{\delta^2 + \beta^2}$$

(bond energy in simple MO theory; in practice *D* is between 3 and 4 eV and thus θ *ca.* $\pi/6$).

$$\begin{cases} \psi_{(I)} = \cos\theta\, p_S + \sin\theta\, p_{(I)} \\ \varepsilon_{(I)} = \alpha_S - D\sin^2\theta \end{cases} \qquad \begin{cases} \psi_{(II)} = \sin\theta\, p_S + \cos\theta\, p_{(II)} \\ \varepsilon_{(II)} = \alpha_S - D\cos^2\theta \end{cases}$$

$$\begin{cases} \psi_{(I)}^* = \sin\theta\, p_S - \cos\theta\, p_I \\ \varepsilon_{(I)}^* = \alpha_S + D\cos^2\theta \end{cases} \qquad \begin{cases} \psi_{(II)}^* = \cos\theta\, p_S - \sin\theta\, p_{(II)} \\ \varepsilon_{(II)}^* = \alpha_S + D\sin^2\theta \end{cases}$$

(I) (II)

Let us now consider the interaction between ψ_i^* and p_o of oxygen. If $-\gamma_i = \langle\psi_i^*|H|p_o\rangle$, we obtain

$$\gamma_{(I)} = \beta/2\sin\theta = D/4\sin\theta\sin 2\theta$$

$$\gamma_{(II)} = D/4\sin 2\theta\cos\theta$$

From the values of relevant integrals, we see immediately that in case (I), the coupling is small (due to $\varepsilon_{(I)}^* - \alpha_o$) and to the smallness of the sulphur contribution to $\psi_{(I)}^*$. In case (II), we can easily obtain the resulting bonding function $\varphi = c\psi_{(II)}^* + dp_o$.

Its energy is

$$E_{(II)} = \alpha_o - \frac{D}{2}\cos^2\theta\sqrt{1 + \sin^2\theta} - 1$$

$$ca.\ \alpha_o - \frac{D}{16}\sin^2 2\theta$$

This gives an overall stabilisation of *ca.* 0.4 eV, *c ca.* $\sin\theta/2$, so that the coefficient of φ on sulphur is $(\frac{1}{4}\sin 2\theta)$.

A similar calculation for (I) would give

$$E_{(I)}\ ca.\ \alpha_o - \frac{D}{16}\frac{\sin^2\theta\sin^2 2\theta}{(\cos 2\theta + \cos^2\theta)}$$

(the stabilisation would be five times smaller in this case).

The results are summarised in Figure 5.

Acknowledgements

The authors are indebted to Dr. B. Gillon for help in the energy calculations and thank Professor J. Lajzerowicz for valuable comments and Dr. S. Sólyom for supplying compound (II). Mmes. G. D'Assenza and J. Allibon are thanked for skillful technical assistance. One of us (L. P.) was helped during part of the work by a grant from the C.N.R.S., France.

References

1 A. Kálmán and L. Párkányi, *Acta Crystallogr.*, 1980, **B36**, 2372.
2 J. A. Kapecki and J. E. Baldwin, *J. Am. Chem. Soc.*, 1969, **91**, 1120.
3 R. Pinel, Y. Mollier, J. P. de Barbeyrac, and G. Pfister-Guillouzo, *C.R. Acad. Sci.*, 1972, **275**, 909.
4 J. P. de Barbeyrac, D. Gonbeau, and G. Pfister-Guillouzo, *J. Mol. Struct.*, 1973, **16**, 103.
5 C. Cohen-Addad, J. M. Savariault, and M. S. Lehmann, *Acta Crystallogr.*, 1981, **B37**, 1703.
6 S. Sólyom, P. Sohár, L. Toldy, A. Kálmán, and L. Párkányi, *Tetrahedron Lett.*, 1977, **48**, 4245.
7 J. R. Allibon, A. Filhol, M. S. Lehmann, S. A. Mason, and P. Simms, *J. Appl. Crystallogr.*, 1981, **14**, 326.
8 M. S. Lehmann and F. K. Larsen, *Acta Crystallogr.*, 1974, **A30**, 580.
9 W. R. Busing and H. A. Levy, ORXFL3, Report ORNL-TM-271, Oak Ridge National Laboratory, Tennessee, 1962.
10 P. Coppens, personal communication.
11 L. Koester and H. Rauch, IAEA Contract 2517/RB, 1981.
12 C. K. Johnson, ORTEP Report ORNL 3794, Oak Ridge National Laboratory, Tennessee, 1965.
13 B. Dawson, *Acta Crystallogr.*, 1964, **17**, 997.
14 R. Hoffman and W. N. Lipscomb, *J. Chem. Phys.*, 1962, **36**, 2179.

Received 9th March 1983; *Paper* 3/374